

ARTICLE OPEN



TMTC1 promotes invasiveness of ovarian cancer cells through integrins $\beta 1$ and $\beta 4$

Ting-Chih Yeh¹, Neng-Yu Lin¹, Chin-Yu Chiu¹, Tzu-Wen Hsu¹, Hsin-Yi Wu², Hsuan-Yu Lin¹, Chi-Hau Chen³ and Min-Chuan Huang¹

© The Author(s) 2023

Ovarian cancer is the most lethal gynecological malignancy and is characterized by peritoneal disseminated metastasis. Although O-mannosyltransferase TMTC1 is highly expressed by ovarian cancer, its pathophysiological role in ovarian cancer remains unclear. Here, immunohistochemistry showed that TMTC1 was overexpressed in ovarian cancer tissues compared with adjacent normal ovarian tissues, and high TMTC1 expression was associated with poor prognosis in patients with ovarian cancer. Silencing TMTC1 reduced ovarian cancer cell viability, migration, and invasion in vitro, as well as suppressed peritoneal tumor growth and metastasis in vivo. Moreover, TMTC1 knockdown reduced cell-laminin adhesion, which was associated with the decreased phosphorylation of FAK at pY397. Conversely, TMTC1 overexpression promoted these malignant properties in ovarian cancer cells. Glycoproteomic analysis and Concanavalin A (ConA) pull-down assays showed that integrins $\beta 1$ and $\beta 4$ were novel O-mannosylated protein substrates of TMTC1. Furthermore, TMTC1-mediated cell migration and invasion were significantly reversed by siRNA-mediated knockdown of integrin $\beta 1$ or $\beta 4$. Collectively, these results suggest that TMTC1-mediated invasive behaviors are primarily through integrins $\beta 1$ and $\beta 4$ and that TMTC1 is a potential therapeutic target for ovarian cancer.

Cancer Gene Therapy (2023) 30:1134–1143; <https://doi.org/10.1038/s41417-023-00625-y>

INTRODUCTION

Ovarian cancer has the highest mortality rate among gynecological malignancies [1]. Most patients are diagnosed at advanced stages when ovarian cancer tumors have metastasized extensively in the peritoneal cavity, resulting in a 5-year survival rate below 50% [2]. Therefore, a deeper understanding of the molecular mechanisms underlying ovarian cancer metastasis is required for the development of novel therapeutic agents to improve patient outcomes.

Integrins, a large family of cell surface proteins that play important roles in epithelial cell-matrix interactions, are heterodimeric molecules consisting of paired α and β subunits. In mammals, 18 α and 8 β subunits have been characterized; the combination of them forms 24 distinct integrins. The integrin-FAK pathway regulates various cellular functions, including adhesion, migration, invasion, survival, growth, and differentiation in normal as well as tumor tissues [3–8]. Moreover, integrins have a great impact on cancer metastasis; therefore, they are appealing targets for cancer therapy.

Glycosylation is the most complex post-translational modification of proteins, which determines the structure and function of numerous secreted and membrane-bound proteins. Protein O-mannosylation, a type of glycosylation conserved from fungi to mammals [9], is the addition of the mannose from dolichol-phosphate mannose (Dol-P-Man) to serine or threonine residues of nascent polypeptides in the endoplasmic reticulum (ER). One type of this reaction is catalyzed by POMT1 and POMT2 with

α -dystroglycan (α -DG) as the main substrate in mammals [10, 11]. The O-Man glycans are crucial in muscle and brain development; its deficiency in α -DG causes a group of congenital muscular dystrophies. Recently, a broad spectrum of O-mannosylated proteins has been identified, including cadherins/protocadherins and plexins, which do not involve POMT1 and POMT2 [12, 13]. Transmembrane and tetratricopeptide repeat containing 1–4 (TMTC1–4) are newly identified enzymes responsible for the O-mannosylation of cadherins and protocadherins [12, 14]. The TMTC-mediated O-Man is not elongated into complex glycans found in POMT1/2-dependent O-Man glycosylation but is instead limited to single O-Man monosaccharide structures [13]. The O-mannosylation of E-cadherin is essential for its correct localization on the cell membrane, and altered O-mannosylation disturbs the assembly of adherens junctions in gastric cancer [15]. With respect to the O-mannosylation of plexins, it appears to be catalyzed by currently unknown enzymes in mammalian cells.

High *TMTC1* mRNA expression is associated with decreased survival of patients with gastric cancer [16]. The Cancer Genome Atlas (TCGA) database showed that *TMTC4* mRNA was overexpressed in prostate cancer tissues compared with normal prostate tissues [17]. Although TMTC-mediated O-mannosylation is conserved in mammalian cells and is expected to play crucial roles in cellular behaviors, the pathophysiological roles of TMTC1–4 in cancers remain largely unknown. In this study, we observed that high TMTC1 expression was associated with poor prognosis in patients with ovarian cancer. Integrins $\beta 1$ and $\beta 4$ were identified

¹Graduate Institute of Anatomy and Cell Biology, College of Medicine, National Taiwan University, Taipei, Taiwan. ²Instrumentation Center, National Taiwan University, Taipei, Taiwan. ³Department of Obstetrics and Gynecology, National Taiwan University Hospital, Taipei, Taiwan. ✉email: chihau@ntuh.gov.tw; mchuang@ntu.edu.tw

Received: 17 January 2023 Revised: 20 April 2023 Accepted: 4 May 2023

Published online: 23 May 2023

as novel protein substrates of TMTC1. Moreover, TMTC1 promoted migration and invasion of ovarian cancer cells by modifying O-mannosylation and activity of integrins β 1 and β 4. Importantly, silencing of TMTC1 was sufficient to inhibit invasiveness and peritoneal metastasis of ovarian cancer cells. Our findings provide novel mechanistic insights into the role of TMTC1 in ovarian cancer pathogenesis.

MATERIALS AND METHODS

Cell lines and culture

Human ovarian cancer cell lines, including ES-2 (ATCC, Manassas, VA, USA), SKOV3 (ATCC, Manassas, VA, USA), and OVTW59 (a kind gift from Dr. P. L. Tong, Department of Obstetrics and Gynecology, National Taiwan University), were maintained in Dulbecco's modified Eagle's medium (DMEM) (Invitrogen, Grand Island, NY, USA) supplemented with 10% fetal bovine serum (Gibco, Gaithersburg, MD, USA). All cells were incubated in a humidified atmosphere of 5% CO₂ and 95% air at 37 °C. All human cell lines have been authenticated using STR profiling within 1 year. All experiments were performed with mycoplasma-free cells.

Antibody generation and immunohistochemistry

Ovarian cancer tissue microarrays (Biomax BC11115c and HOvaC154Su01) were purchased from US Biomax, Inc. (Rockville, MD, USA) for immunohistochemical staining. The tissue microarrays were incubated with an anti-TMTC1 polyclonal antibody (in-house) at 2 μ g/mL at 4 °C overnight. The specific immunostaining was visualized with 3, 3'-diaminobenzidine Quanto Chromogen in the UltraVision™ Quanto Detection System (Thermo Fisher Scientific, San Jose, CA, USA). All sections were counterstained with hematoxylin for 1 s. The intensity of TMTC1 expression was scored as 0 (negative), 1 (faint), 2 (moderate), and 3 (strong).

The in-house anti-TMTC1 polyclonal antibody was raised by immunizing rabbits with recombinant TMTC1. The pGEX-4T-1 plasmid with inserted TMTC1 was constructed and transformed into *Escherichia coli* BL21 competent cells. The recombinant TMTC1 expression was induced for 16 h at 20 °C by adding 1 mM isopropyl- β -D-thiogalactoside when the A_{600nm} value of the cultures was 0.4 to 0.5. The soluble fraction and the inclusion body were separated using a 9% SDS-PAGE gel and stained with Coomassie brilliant blue (Supplementary Fig. S1A). The recombinant TMTC1 (65.8 kDa) was transferred to a PVDF membrane and incubated with the anti-serum to purify the anti-TMTC1 polyclonal antibody. Then, the anti-TMTC1 polyclonal antibody on the PVDF membrane was eluted for immunohistochemistry (Supplementary Fig. S1B). Western blots confirmed that HA-tagged TMTC1 was detected by anti-TMTC1 polyclonal antibody (Supplementary Fig. S1C).

Real-time RT-PCR analysis

Total RNA was isolated using the TRIzol reagent (Invitrogen, Grand Island, NY, USA), and cDNA was synthesized using the High Capacity cDNA Reverse Transcription Kit (Applied Biosystems, Carlsbad, CA, USA). The cDNA was subjected to real-time RT-PCR using primers for TMTC1 (5'-TGTGTCTCAGAGGACCGGAT-3' and 5'-GGTTTCAGCTGGAGAGCCTT-3') or GAPDH (5'-TGAAGTCTGGAGTCAACGGATT-3' and 5'-CCTGGAAGATGGTATGGGATT-3').

MTT assay

Cell viability was determined using the 3-(4,5-dimethylthiazol-2-yl)-2,5-diphenyltetrazolium bromide (MTT) assay. In summary, 10 μ l of 5 mg/ml MTT (Sigma, St. Louis, MO, USA) was added to each well in a 96-well plate and incubated at 37 °C for 3 h. Next, the MTT formazan crystals formed by the metabolically viable cells were dissolved in 100 μ l of 0.01 N HCl with 10% SDS. Finally, the absorbance was measured at dual wavelengths of 550 and 630 nm using a microplate reader.

Transfection and plasmid construction

The pRL-TK was an empty plasmid for control. TMTC1 plasmid was pRL-TK plasmid containing human full-length TMTC1 sequence. The TMTC1 and control empty pRL-TK constructs were acquired from the Biomedical Resource Core of the First Core Laboratory, College of Medicine, National Taiwan University. TMTC1 overexpression was investigated by first transfecting ovarian cancer cells with the TMTC1/pRL-TK plasmids using Lipofectamine 3000 (Invitrogen, Grand Island, NY, USA). An empty pRL-TK

plasmid was used as the mock transfection. In contrast, TMTC1 was knocked down by transfecting the cells with 10 nM siRNA using Lipofectamine RNAiMAX (Invitrogen, Grand Island, NY, USA) for 48 h. The siRNA used was the control siRNA (5'-CAA CCU CAG CCA UGU CGA CUG GUU U-3') of medium GC content or two siRNAs oligonucleotides against TMTC1, siTMTC1-1 (5'-UGU CAC CUU UGG GAG CAC UGU AUU A-3') and siTMTC1-3 (5'-ACG GUG UUU GGA GUG UGC UUG GUU U-3') (Invitrogen, Grand Island, NY, USA). In addition, siRNAs against ITGB1 (si-ITGB1-1, 5'-CCU AAG UCA GCA GUA GGA ACA UUA U-3' and si-ITGB1-2, 5'-UGC GAG UGU GGU GUC UGU AAG UGU A-3'), ITGB4 (si-ITGB4-1, 5'-GCC UAC UGC ACA GAC GAG AUG UUC A-3' and si-ITGB4-2, 5'-CCG GAU GCU UAU UGA GAA CCU U-3') were synthesized. The pLKO/TMTC1-shRNA plasmid (TRCN147171) and non-targeting pLKO plasmids (TRCN208001) were purchased from National RNAi Core Facility (Academia Sinica, Taipei, Taiwan). The oligo sequence of pLKO/TMTC1-shRNA is CCGGCGATTACAAGAAGTTCGAGAAGTTCGAGTCTCGAACTCTTGTAAATCGTTTTTTG. Target sequence of TMTC1 is CGATTACAAGAAGTTCGAGAA. Stable knockdown was performed with the shRNA construct in pLKO.1 plasmid using a lentivirus-based infection system. On the other hand, stable overexpression was performed with lentiviral transfer vector, pLAS2w.Ppuro-TMTC1-HA or pLAS2w.Ppuro, using a lentivirus-based infection system. Stable knockdown and overexpression cells were selected with 500 ng/ml puromycin for 14 days. The knockdown of TMTC1 was confirmed by real-time RT-PCR. To establish stable overexpression of TMTC1 in cells, we utilized a lentivirus-based infection system and infected cells with pLAS2w.Ppuro-TMTC1-HA or pLAS2w.Ppuro lentiviral transfer vector. Subsequently, the cells were subjected to puromycin selection at a concentration of 500 ng/ml for a duration of 14 days to obtain the TMTC1 stable overexpressing cell population.

Transwell migration assay and Matrigel invasion assay

Transwell migration assay was performed using chambers with 8- μ m membranes (Corning Incorporated, Corning, NY, USA). The Transwell chambers were coated with Matrigel (Corning Incorporated, Corning, NY, USA) for the Matrigel invasion assay. Cells were detached and suspended in a serum-free medium and seeded on the upper chamber. A medium with 10% FBS in the lower chamber was used as the chemoattractant. After 24 h of incubation, the cells on the lower surface of the chamber were stained with crystal violet (Sigma, St. Louis, MO, USA) in 20% (v/v) methanol and counted under a microscope. The experiments were performed in triplicates, and four fields of each transwell were analyzed.

Adhesion assay

Collagen I, collagen IV, fibronectin, laminin, or control bovine serum albumin (BSA) at 5 μ g/ml in PBS were coated on 6-wells plates for 3 h and blocked with 1% BSA in PBS at 4 °C overnight. Cells (4×10^5) in 1 ml serum-free DMEM medium per well were allowed to attach to coated plates at 37 °C for 20 min. Then, the adhered cells were counted manually under an inverted microscope. In addition, the cells were collected for western blot analysis.

LC-MS/MS analysis and database search

The extracellular domain of integrins β 1 and β 4 expressed by HEK293 were purchased from Sino Biological for high-energy collision activated dissociation (HCD) and/or electron-transfer/higher-energy collision dissociation (ETHcD) mass spectrometry. LC-MS/MS analysis with HCD and/or ETHcD fragmentation was conducted on an Orbitrap Fusion Lumos Tribrid quadrupole-ion trap-Orbitrap mass spectrometer (Thermo Fisher Scientific, San Jose, CA, USA) equipped with a nanospray interface. Peptides were separated on an Ultimate system 3000 nanoLC system (Thermo Fisher Scientific, Bremen, Germany) linked to a mass spectrometer. In summary, peptides were loaded onto a 75- μ m ID, 25-cm C18 Acclaim PepMap NanoLC column (Thermo Scientific, San Jose, CA, USA) packed with 2- μ m particles with 100-Å pores. Mass spectrometry analysis was performed in a data-dependent mode with Full-MS with a resolution of 120,000 at m/z = 200, AGC target 5e5, maximum injection time of 50 msec. HCD-MS/MS (resolution of 15,000) of the most intense ions in 3 s was used to fragment multiply charged ions within a 1.4 Da isolation window at a normalized collision energy of 32%. AGC target 5e4 was set for MS/MS analysis with previously selected ions dynamically excluded for 180 s. Max injection time 50 ms. The ETD reaction time was set to 250 ms for ETHcD (resolution of 60,000). HCD supplemental activation was enabled with normalized collision energy set to 15%. (calculation based on precursor m/z and charge state). The AGC target was set to 4e5 for ETHcD.

Protein identification was performed by searching the raw MS/MS data against the Uniprot human database using the Mascot search algorithms (version 2.3) via the Proteome Discoverer package (version 2.2, Thermo Scientific, San Jose, CA, USA). The mass spectrometry proteomics data have been deposited to the ProteomeXchange Consortium via the PRIDE [18] partner repository with the dataset identifier PXD037907.

ConA pull-down assay

The changes in O-mannose were analyzed by first treating 250 µg or more of total cell lysates with PNGase F (New England Biolabs, Ipswich, MA, USA) to remove the N-glycans. Then, the cell lysates were incubated with ConA-agarose beads (Vector Laboratories, Burlingame, CA, USA) at 4°C overnight. Next, the ConA-agarose beads were washed with PBS five times to remove unbound proteins and subjected to Western blotting. For cell surface biotinylation, OVTW59 cells were transfected with control siRNA (siControl) or *TMTC1* siRNA (si*TMTC1*-1). After using EZ-Link Sulfo-NHS-Biotin (Thermo Fisher Scientific, San Jose, CA, USA) to biotinylate surface molecules, cell lysates were treated with PNGase F to remove N-glycans. Then, ConA-agarose beads were used to pull down glycoproteins with mannoses. The biotinylated glycoproteins were detected using streptavidin-HRP and an ECL kit.

Western blot analysis

Cell lysates were extracted from cell pellets in NP40 buffer. The proteins were separated on a 9% SDS-PAGE gel and transferred onto a PVDF membrane. The membrane was blocked in 5% BSA (Bio-Rad, Hercules, CA, USA) at room temperature for 1 h and incubated with a primary antibody against integrin β4 (Cell Signaling Technology, Danvers, MA, USA), integrin β1 (BD Biosciences, San Jose, CA, USA), p-FAK (Cell Signaling Technology, Danvers, MA, USA), FAK (Santa Cruz Biotechnology, Santa Cruz, CA, USA), *TMTC1* (in-house) or GAPDH (Santa Cruz Biotechnology, Santa Cruz, CA, USA) at 4°C overnight. Then, the membranes were incubated with horseradish peroxidase-conjugated secondary antibodies, and the protein bands were detected using ECL reagents (GE Healthcare Life Sciences, Pittsburgh, PA, USA).

Peritoneal metastasis assay

Female BALB/cAnN.Cg-Foxn1nu/CrI Narl nude mice aged between 5 and 7 weeks were procured from the National Laboratory Animal Center, Taiwan. They are in general SPF conditions. The nude mice were fed a normal diet LabDiet5010. The water for nude mice is sterilized reverse osmosis (RO) water at the Animal Center of National Taiwan University College of Medicine. For peritoneal injection, we used 1 mL syringes and 24 G needles. ES-2 and SKOV3 cells were mixed in a 1:1 ratio with Matrigel™ Basement Membrane Matrix (Corning Incorporated, Corning, NY, USA), and subsequently, either 5×10^6 ES-2 cells or 1×10^7 SKOV3 cells were injected intraperitoneally into the nude mouse. The formation of metastatic nodules was assessed by measuring their numbers and weights 15 or 40 days post-injection of ES-2 or SKOV3 cells, respectively, after which the mice were sacrificed. All animal procedures were conducted following the guidelines approved by the Animal Ethics Committee.

Statistical analysis

Statistical analyses were performed using the SPSS 22.0 (SPSS, Chicago, IL, USA) statistical software package. The Student's *t*-test, ANOVA and Kaplan–Meier plotter were used to analyze experiments. Data were shown as means ± SD, and two-sided $P < 0.05$ is considered statistically significant.

RESULTS

TMTC1 expression is upregulated in ovarian cancer and higher *TMTC1* expression is associated with poorer prognosis in patients with ovarian cancer

Initially, to discover the expression pattern of *TMTC1* in various cancer tissues, we searched TCGA database and used RNA-seq data from 17 cancer types for comparisons. We found that *TMTC1* expression levels in serous type ovarian adenocarcinomas were significantly higher than those in other tumors (Fig. 1A). We then examined the prognostic value of *TMTC1* expression in a public database Kaplan–Meier plotter (KM plotter) based on microarray data from ovarian cancer patients. The Kaplan–Meier survival

analysis showed that ovarian cancer patients with high *TMTC1* expression had poorer survival (Fig. 1B). In addition, we examined *TMTC1* levels in a tissue microarray (Biomax BC11115c) using immunohistochemical staining. The *TMTC1* levels were scored from 0 to 3 (Fig. 1C). Samples were then classified as either low (0 and 1) or high (2 and 3) for *TMTC1* protein expression. The results showed that *TMTC1* was frequently overexpressed in cancerous ovarian specimens compared with normal tissues (Fig. 1D). We further used the clinical samples from another tissue microarray (Biomax HOvaC154Su01) to analyze the effect of *TMTC1* on the survival of ovarian cancer patients. Consistently, the Kaplan–Meier analysis confirmed that high *TMTC1* expression was significantly associated with poor overall survival (Fig. 1E). Notably, the multivariate analysis showed that in addition to lymph node and distant metastasis, *TMTC1* is an independent prognostic factor for poor prognosis ($P = 0.03$) (Supplementary Table S1). These findings suggest that *TMTC1* expression is elevated in cancerous ovarian tissues and that high *TMTC1* expression predicts poor survival in patients with ovarian cancer.

TMTC1 promotes malignant phenotypes in ovarian cancer cells

To investigate the effects of *TMTC1* on malignant cell behaviors in vitro, cell viability, migration and invasion were assessed in ovarian cancer cells. First, we analyzed endogenous levels of *TMTC1* in ovarian cancer cells. SKOV3 cells had the highest *TMTC1* level followed by OVTW59 cells, whereas ES-2 cells had the lowest *TMTC1* level (Supplementary Fig. S2). Therefore, we chose SKOV3 and OVTW59 cells for *TMTC1* knockdown experiments and ES-2 cells for *TMTC1* overexpression experiments. *TMTC1* knockdown or overexpression was confirmed using real-time RT-PCR analysis (Fig. 2A). The average knockdown efficiencies of *TMTC1* in OVTW59 and SKOV3 cells were 79.2% and 75.1%, respectively. The overexpression of *TMTC1* in ES-2 cells was 762.5 times compared with the control. The results of MTT assays indicated that *TMTC1* knockdown decreased, whereas *TMTC1* overexpression increased, cell viability (Fig. 2B). The transwell migration assay showed that knockdown of *TMTC1* decreased migration in both OVTW59 and SKOV3 cells, whereas *TMTC1* overexpression increased migration in ES-2 cells (Fig. 2C). The Matrigel invasion assay indicated that *TMTC1* knockdown suppressed invasion in OVTW59 and SKOV3 cells (Fig. 2D). By contrast, *TMTC1* overexpression enhanced ES-2 cell invasion. Moreover, *TMTC1* knockdown decreased migration and invasion in ES-2 cells, which is consistent with the findings in SKOV3 and OVTW59 cells (Supplementary Fig. S3). These findings suggest that *TMTC1* promotes the viability, migration and invasion of ovarian cancer cells.

TMTC1 enhances cell-laminin adhesion in ovarian cancer cells

Given that adhesion ability is involved in migration and invasion [19], we next investigated whether *TMTC1* modulated cell adhesion to extracellular matrix (ECM) proteins, including fibronectin, laminin, collagen I, and collagen IV. The results showed that *TMTC1* knockdown significantly decreased cell adhesion to laminin in OVTW59 cells (Fig. 3A). Moreover, *TMTC1* knockdown also decreased cell-laminin adhesion in SKOV3 cells. In contrast, *TMTC1* overexpression increased cell-laminin adhesion in ES-2 cells (Fig. 3B). Since cell-laminin adhesion enhances FAK phosphorylation, we analyzed FAK phosphorylation at pY397 in ovarian cancer cells seeded on laminin-coated plates. We quantified the pFAK and total FAK from Western blots in ovarian cancer cells. The results showed that *TMTC1* knockdown decreased, whereas *TMTC1* overexpression increased, FAK phosphorylation (Supplementary Fig. S4). As expected, *TMTC1* knockdown decreased FAK phosphorylation while OVTW59 and SKOV3 cells adhered to laminin (Fig. 3C). In contrast, *TMTC1* overexpression enhanced FAK phosphorylation in ES-2 cells. These

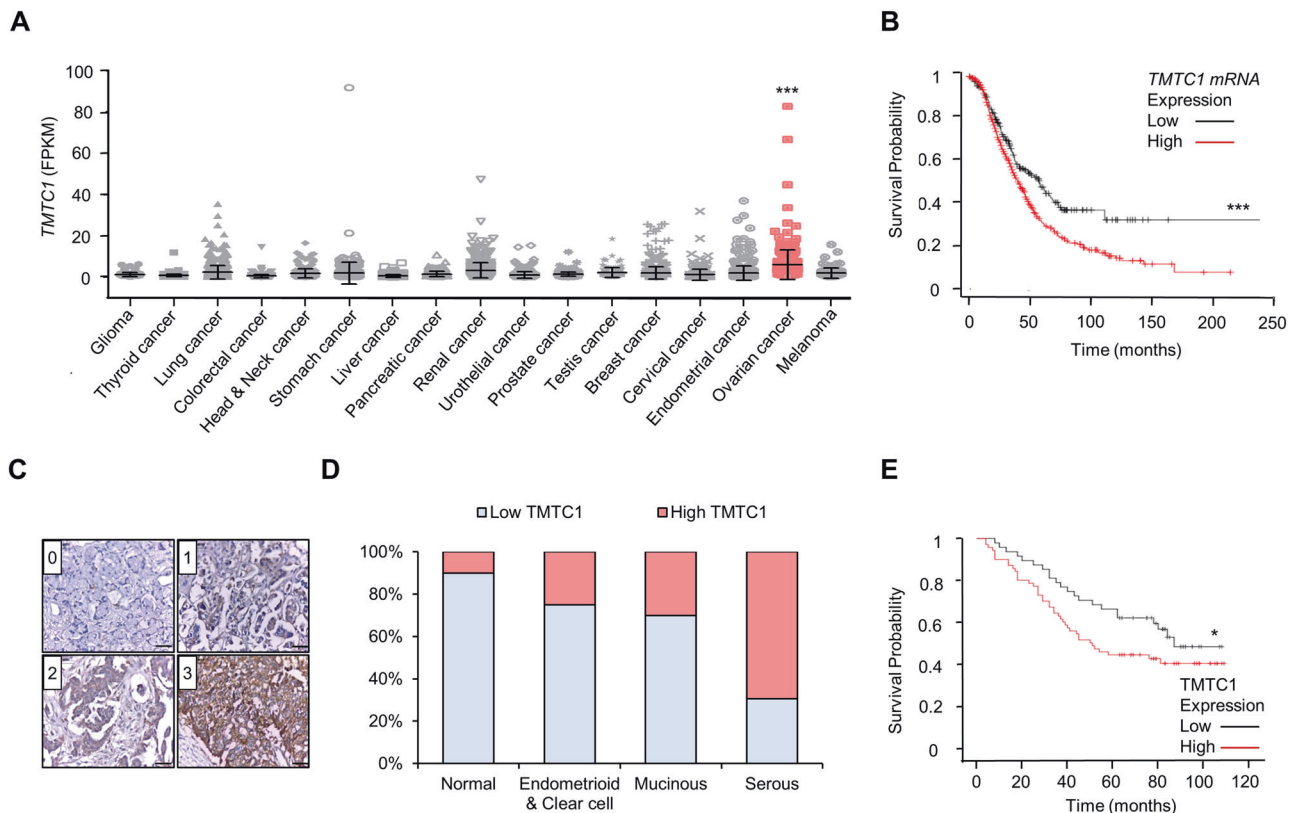


Fig. 1 TMTTC1 expression is upregulated in ovarian cancer and higher TMTTC1 expression is associated with poorer prognosis in patients with ovarian cancer. **A** TMTTC1 expression in various cancers from the TCGA database. The tumor tissues of 373 serous ovarian cancer patients had higher TMTTC1 mRNA levels than glioma ($n = 153$), thyroid cancer ($n = 501$), lung cancer ($n = 994$), colorectal cancer ($n = 597$), head and neck cancer ($n = 499$), stomach cancer ($n = 354$), liver cancer ($n = 365$), pancreatic cancer ($n = 176$), renal cancer ($n = 877$), urothelial cancer ($n = 406$), prostate cancer ($n = 494$), testis cancer ($n = 134$), breast cancer ($n = 1075$), cervical cancer ($n = 291$), endometrial cancer ($n = 541$), and melanoma ($n = 102$). Fragments Per Kilobase of exon model per Million mapped fragments (FPKM) for each gene was used for quantification of expression with a detection threshold of 1 FPKM. Data were analyzed using one-way ANOVA. $***P < 0.001$. **B** Analysis of overall survival using the Kaplan-Meier plotter. Expression ranges of the probes are from 3 to 4993. Kaplan-Meier plotter takes the probe value of 201 as the cut point between high and low expression. The median survival of low expression cohort is 57.1 months and high expression cohort is 40 months. Kaplan-Meier plotter analyzes all histological subtypes with all grades. The patient numbers for high (red) and low (black) TMTTC1 expression are 444 and 211, respectively. $***P < 0.001$. **C** Scoring TMTTC1 levels from 0 to 3 in ovarian cancer tissues immunostained with an anti-TMTTC1 antibody. Scale bar, 0.5 mm. **D** Immunohistochemistry of TMTTC1 levels in ovarian tumors ($n = 90$), including 62 serous carcinomas, 10 mucinous carcinomas, 3 endometrioid carcinomas, 5 clear cell carcinomas, and adjacent normal ovary tissues ($n = 10$). **E** Kaplan-Meier survival curve for overall survival. TMTTC1 expression in ovarian cancer tissue microarrays was divided into the low (0–1; $n = 43$) and high (2–3, $n = 73$) groups. The data exclude cases of specimens from metastatic sites, rare histologic types, and missing data, and include cases of 57 high-grade serous, 14 low-grade serous, 30 mucinous, 13 endometrioid, and 2 clear cell types. $*P < 0.05$.

results suggest that TMTTC1 enhances cell-laminin adhesion and the downstream FAK signaling pathway in ovarian cancer cells.

TMTTC1 modifies O-mannosylation of integrins $\beta 1$ and $\beta 4$ in ovarian cancer cells

To unravel the underlying mechanism of TMTTC1-mediated phenotypic changes in ovarian cancer cells, we identified the protein substrates of TMTTC1 using a glycoproteomic approach. Because ConA can bind N-glycans with glucoses and mannoses, cell lysates were treated with PNGase F to remove the N-glycans. Thus, TMTTC1-mediated changes in O-Man can be detected by performing the ConA pull-down assay with control or TMTTC1 knockdown cells. We found that TMTTC1 knockdown in OVTW59 cells decreased the amount of cell surface proteins pulled down by the ConA-agarose beads (Fig. 4A), suggesting that ConA can recognize TMTTC1 protein substrates after the removal of N-glycans. Next, we used ConA-agarose beads to pull down the PNGase F-treated proteins in OVTW59 cells transfected with control or TMTTC1 siRNA and then performed LC-MS/MS analysis. The results uncovered 17 proteins in the secretory pathway with decreased ConA binding (>2 -fold change) in TMTTC1 knockdown cells

(Supplementary Table S2). Cadherins/protocadherins are known for TMTTC1-4 protein substrates. Our MS proteomics data showed that ConA binding to protocadherin 7 was slightly decreased to 0.87 fold in TMTTC1 knockdown cells (Supplementary Table S3). The O-mannosylation site in protocadherin 7 was confirmed to be S656 of peptide 650-ENLQPN^SPVGMVTVMADKGR-670 (Supplementary Fig. S5). Moreover, the BioPlanet database showed that the functional pathways of the 17 proteins were most closely related to integrin family cell surface interactions, followed by support of platelet aggregation by Eph kinases and ephrins (Supplementary Table S4).

Our data showed that TMTTC1 enhanced cell-laminin adhesion. Among the potential protein substrates of TMTTC1, integrins $\beta 1$ and $\beta 4$ are laminin receptors [20]. To confirm the existence of O-mannosylation on integrins $\beta 1$ and $\beta 4$, we analyzed their extracellular domains expressed by HEK293 cells using HCD or EThcTD mass spectrometry. The results of HCD-MS/MS showed that seven O-mannosylated sites, including S224, S263, S327, T333, S468, S474, and S587/S594, were identified in integrin $\beta 1$ (Supplementary Fig. S6). Besides, S387 was identified to be O-mannosylated on integrin $\beta 4$ using

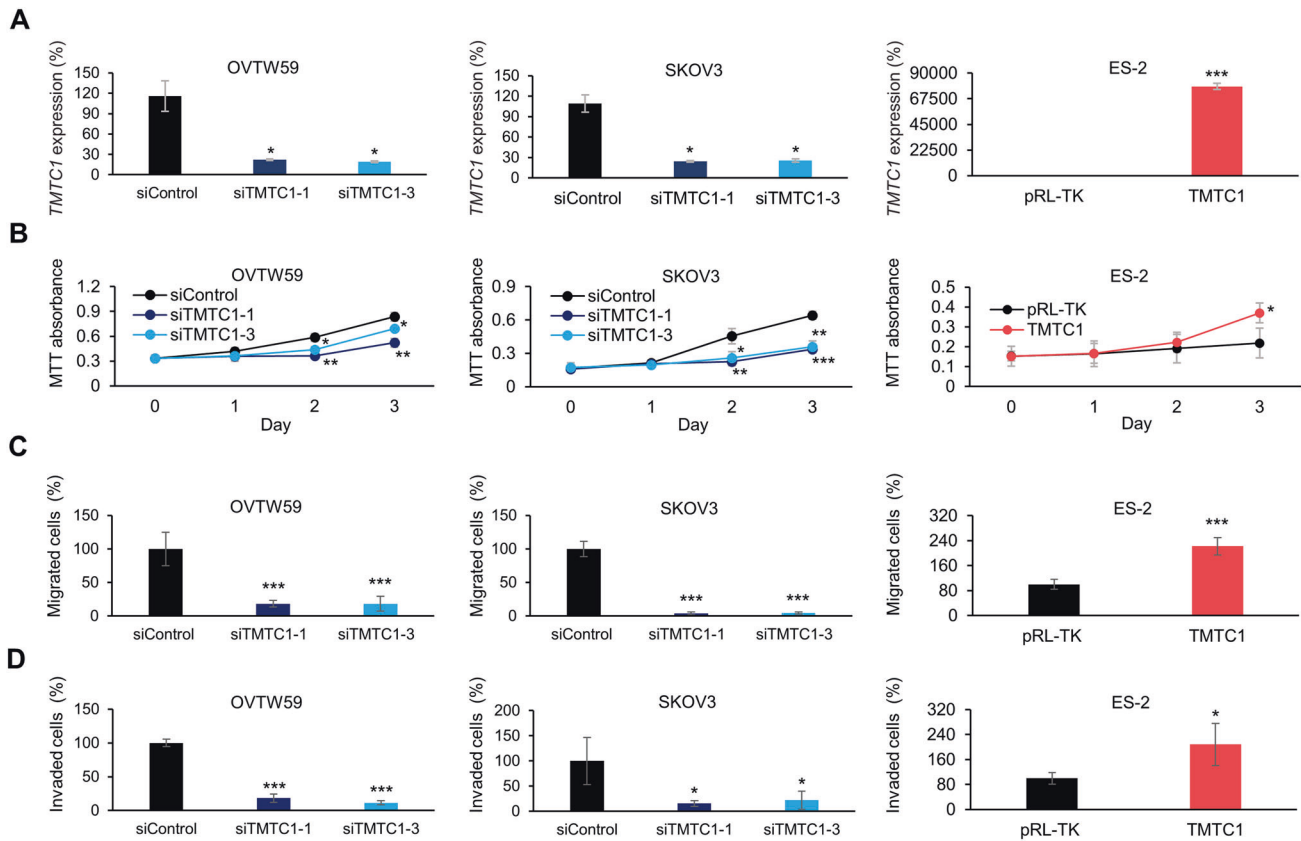


Fig. 2 **TMTC1 promotes malignant phenotypes in ovarian cancer cells.** **A** TMTC1 knockdown or overexpression in ovarian cancer cells. OVTW59 and SKOV3 cells were transfected with non-targeting siRNA (siControl) or two independent siRNAs against TMTC1 (siTMTC1-1 and siTMTC1-3) for 48 h. ES-2 cells were transfected with empty pRL-TK or pRL-TK/TMTC1 plasmid for 48 h. The relative transcript levels of TMTC1 were measured by real-time RT-PCR, and the results were normalized to GAPDH mRNA levels. Representative results from three independent experiments were shown. **B** Effects of TMTC1 on cell viability. *TMTC1* was knocked down in OVTW59 and SKOV3 cells using two independent siRNAs, siTMTC1-1 and siTMTC1-3. A non-targeting siRNA (siControl) was used as the control. TMTC1 was overexpressed in ES-2 cells using pRL-TK/TMTC1 (TMTC1). An empty pRL-TK plasmid was used for control. First, 1×10^3 OVTW59, SKOV3, and ES-2 cells were seeded into each well of 96-well plates. Viable cells were measured using the MTT assay at different time points, as indicated. $n = 3$. **C** Effects of TMTC1 on migration. After transfection for 48 h, 3.5×10^4 OVTW59, 1×10^4 SKOV3, and 1×10^4 ES-2 cells were seeded for the transwell migration assay. In the lower chamber, 10% FBS was used as a chemoattractant. After incubation for 24 h, migrated cells were counted from 4 fields under an inverted microscope. Representative results from three independent experiments were shown. **D** Effects of TMTC1 on cell invasion. After transfection for 48 h, 3.5×10^4 OVTW59, 1×10^4 SKOV3, and 1×10^4 ES-2 cells were seeded for the Matrigel invasion assay. After incubation for 24 h, invaded cells were counted. Representative results from three independent experiments were shown. Data were analyzed using the Student's *t*-test. Data are presented as mean \pm SD ($n = 3$). * $P < 0.05$; ** $P < 0.01$; *** $P < 0.001$.

ETHcD-MS/MS analysis (Supplementary Fig. S7). Next, we investigated the role of integrins $\beta 1$ and $\beta 4$ in TMTC1-mediated effects. As expected, we found that *TMTC1* knockdown decreased ConA binding to integrins $\beta 1$ and $\beta 4$ in OVTW59 and SKOV3 cells (Fig. 4B). For more information, we quantified the integrins $\beta 1$ and $\beta 4$ pulled down by ConA-agarose beads and their changes in ovarian cancer cells (Supplementary Fig. S8). The statistic results showed that TMTC1 knockdown indeed decreased ConA binding to integrins $\beta 1$ and $\beta 4$ but did not significantly alter their levels in OVTW59 cells. In contrast, *TMTC1* overexpression increased ConA binding to integrins $\beta 1$ and $\beta 4$ in ES-2 cells. These findings suggest that TMTC1 can modify the O-mannosylation of integrins $\beta 1$ and $\beta 4$ in ovarian cancer cells. We found that EPHA2 was one of potential TMTC1 protein substrates by our mass spectrometric analysis in OVTW59 cells. However, our results from human phospho-RTK array analysis showed that *TMTC1* knockdown had no significant effect on phospho-RTK levels including EPHA2 (Supplementary Fig. S9), suggesting that EPHA2 did not play an important role in the TMTC1-mediated malignant phenotypes.

Next, we examined whether the α subunits of laminin-binding integrins could be O-mannosylated by TMTC1. Four integrins $\alpha 3\beta 1$, $\alpha 6\beta 1$, $\alpha 7\beta 1$ and $\alpha 6\beta 4$ recognize laminins as their extracellular ligands [20]. We analyzed the levels of α subunits of integrins, $\alpha 3$, $\alpha 6$ and $\alpha 7$, in ovarian cancer cells and found that integrins $\alpha 3$ and $\alpha 6$ were expressed at much higher levels than integrin $\alpha 7$ (Fig. 4C). Next, we performed the ConA pull-down assay and found that *TMTC1* knockdown did not significantly affect the amount of integrins $\alpha 3$ and $\alpha 6$ recognized by ConA (Fig. 4D).

To investigate whether the TMTC1-modified O-mannosylation could modulate heterodimerization of integrin α and β , we performed co-immunoprecipitation assays in ES-2 and SKOV3 cells. We found that *TMTC1* overexpression slightly increased the association of integrin $\alpha 6$ and $\beta 1$, whereas *TMTC1* knockdown decreased. (Supplementary Fig. S10).

A previous study on POMT2 target proteins in gastric cancer has shown the existence of a coordinated interplay between O-mannosylation and N-glycosylation pathway [15]. The transcript levels of MGAT5 and POMT2 showed an inverse relationship. Our real-time RT-PCR data showed that TMTC1 knockdown or

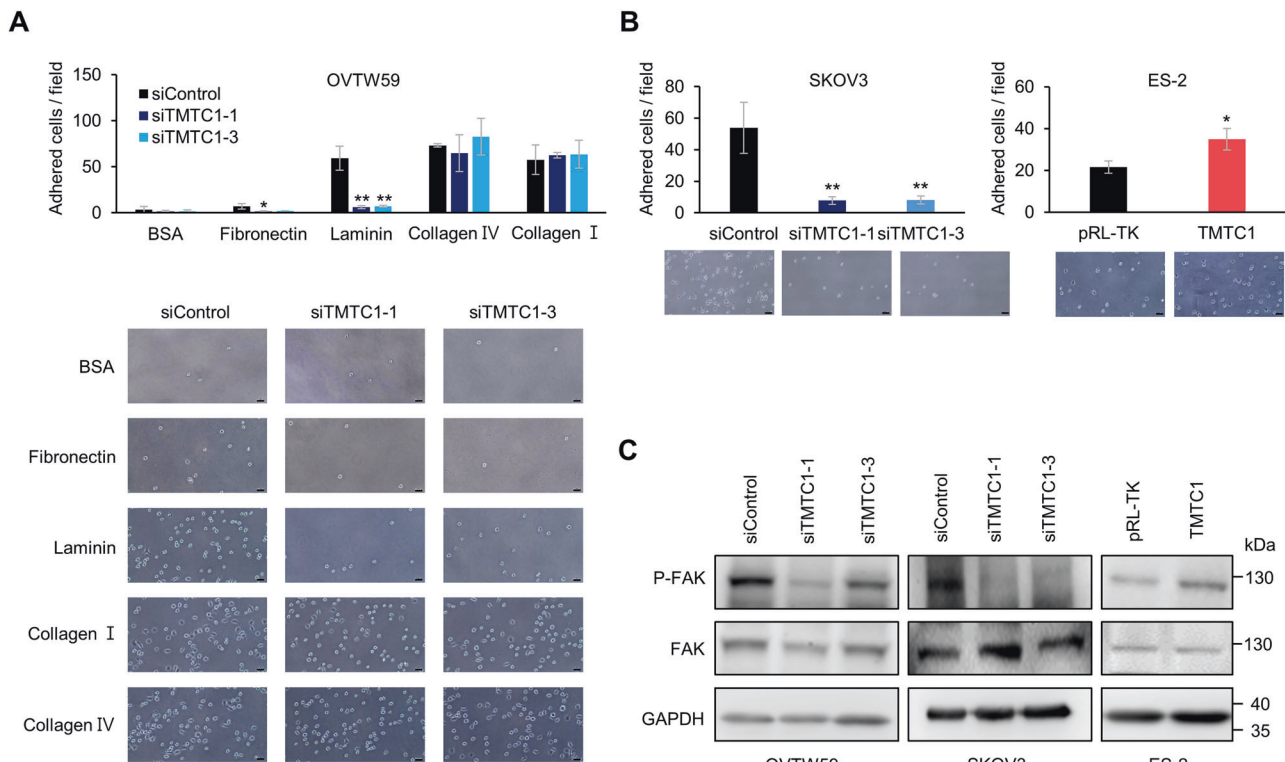


Fig. 3 TMTc1 enhances cell-laminin adhesion in ovarian cancer cells. **A** Cell-ECM adhesion assay. TMTc1 knockdown OVTW59 cells were seeded into 6-well plates coated with 5 $\mu\text{g}/\text{mL}$ laminin, collagen I, collagen IV, or fibronectin; BSA was used as a control. After 20 min of incubation at 37 $^{\circ}\text{C}$, adhered cells were counted in 4 fields under a microscope. Representative images were shown at the lower panel. Representative results from three independent experiments were shown. Data were analyzed using the Student's *t*-test. * $P < 0.05$; ** $P < 0.01$. **B** Cell-laminin adhesion assay. SKOV3 cells with *TMTc1* knockdown and ES-2 cells with TMTc1 overexpression were seeded into 6-well plates coated with 5 $\mu\text{g}/\text{mL}$ laminin. Adhered cells were counted in 4 fields under a microscope. Representative images were shown at the lower panel. Representative results from three independent experiments were shown. Results are presented as mean \pm SD ($n = 3$). Data were analyzed using the Student's *t*-test. * $P < 0.05$; ** $P < 0.01$. **C** Effects of TMTc1 on laminin-mediated tyrosine phosphorylation of FAK. OVTW59 and SKOV3 cells with *TMTc1* knockdown and ES-2 cells with TMTc1 overexpression were plated onto culture plates coated with 5 $\mu\text{g}/\text{mL}$ of laminin in serum-free DMEM. Changes in FAK phosphorylation (pY397) were analyzed using Western blotting. GAPDH was an internal control.

overexpression did not significantly alter the mRNA expression of *MGAT5* (Supplementary Fig. S11).

Integrins $\beta 1$ and $\beta 4$ play a role in the TMTc1-mediated migration and invasion of ovarian cancer cells

Next, we investigated the role of integrin $\beta 1$ or integrin $\beta 4$ in the TMTc1-regulated phenotypes of ovarian cancer cells. Specifically, integrin $\beta 1$ or integrin $\beta 4$ was knocked down using two independent siRNAs in OVTW59 cells with TMTc1 knockdown or ES-2 cells with TMTc1 overexpression (Supplementary Fig. S12). The results showed that shRNA-mediated TMTc1 knockdown inhibited migration and invasion of OVTW59 cells (Fig. 5A). ITGB1 siRNAs dramatically suppressed migration and invasion in both control and TMTc1 knockdown cells, indicating that integrin $\beta 1$ plays a critical role in OVTW59 migration and invasion. Moreover, we observed that the difference in the ability of migration and invasion between control and TMTc1 knockdown was decreased when these cells were treated with ITGB1 siRNAs. We next examined the effect of ITGB1 siRNAs on the migration and invasion of control and TMTc1 overexpressing ES-2 cells. The results showed that ITGB1 siRNAs dramatically suppressed migration and invasion in both control and TMTc1 knockdown cells (Fig. 5B). Notably, the increase of TMTc1-mediated migration and invasion was almost completely blocked. Together with the finding that TMTc1 can regulate cell-laminin adhesion and FAK activity (Fig. 3), these results suggest that integrin $\beta 1$ is involved in the TMTc1-mediated migration and invasion in ovarian cancer cells. To evaluate the contribution of integrin $\beta 4$ in TMTc1-

mediated migration and invasion, we performed similar experiments as described above except using ITGB4 siRNAs. The results showed that ITGB4 siRNAs could also suppress migration and invasion in both control and TMTc1 knockdown cells (Fig. 5C), indicating that integrin $\beta 4$ also plays an important role in OVTW59 migration and invasion. The difference in the ability of migration and invasion between control and TMTc1 knockdown was decreased by ITGB4 siRNAs (Fig. 5C). Moreover, the increase of TMTc1-mediated migration and invasion was almost completely blocked by ITGB4 siRNAs in ES-2 cells (Fig. 5D). These results suggest that integrin $\beta 4$ is also involved in the TMTc1-mediated migration and invasion in ovarian cancer cells. Taken together, integrins $\beta 1$ and $\beta 4$ are needed for the TMTc1-mediated migration and invasion of ovarian cancer cells.

TMTc1 promotes peritoneal tumor growth and metastasis in vivo

Peritoneal dissemination is the most frequently metastatic pattern of ovarian cancer [21]. Thus, we assessed the effect of TMTc1 on peritoneal tumor growth and metastasis. First, we established stable transfectants of ES-2 cells overexpressing TMTc1 with an HA tag (Fig. 6A). Then, these ES-2 cells were injected into nude mice intraperitoneally. The results showed that TMTc1 overexpression increased tumor weights and the number of tumor nodules in the peritoneal cavity (Fig. 6B, C). Furthermore, we established stable transfectants of SKOV3 cells using *TMTc1* shRNA and injected these cells into nude mice intraperitoneally. TMTc1 knockdown was confirmed using real-time RT-PCR analysis

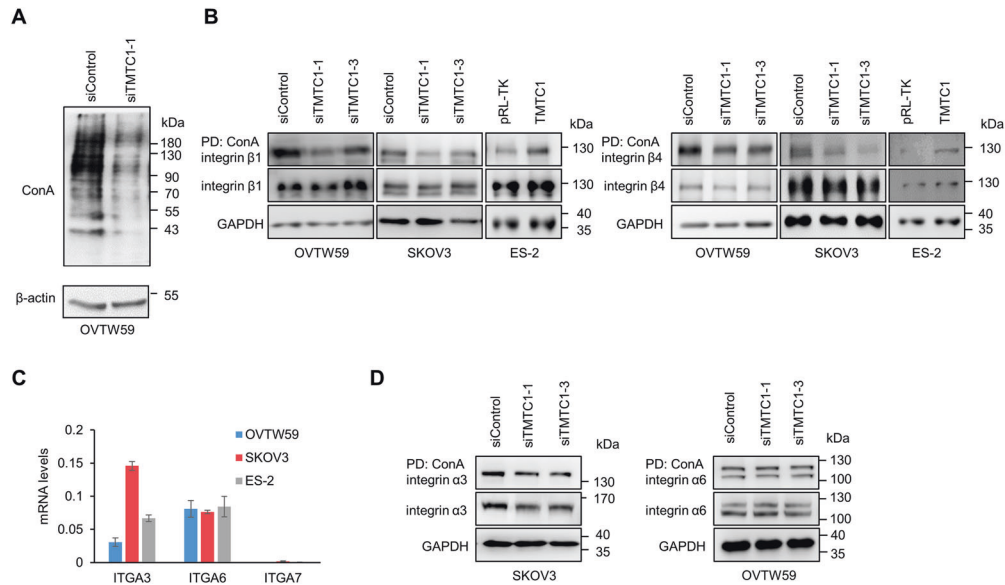


Fig. 4 *TMTc1* modifies O-mannosylation of integrins $\beta 1$ and $\beta 4$ in ovarian cancer cells. **A** ConA pull-down assay. OVTW59 cells were transfected with control siRNA (siControl) or *TMTc1* siRNA (siTMTc1-1). After surface biotinylation, cell lysates were treated with PNGase F to remove N-glycans. Then, ConA-agarose beads were used to pull down glycoproteins with mannoses. The biotinylated glycoproteins were detected using streptavidin-HRP and an ECL kit. **B** ConA pull-down assay of integrin $\beta 1$ and $\beta 4$. *TMTc1* was knocked down with siRNAs in OVTW59 and SKOV3 cells. *TMTc1* was overexpressed in ES-2 cells. Cell lysates were treated with PNGase F and pulled down with ConA-agarose beads. GAPDH was used as a loading control. **C** The mRNA levels of *ITGA3* (integrin $\alpha 3$), *ITGA6* (integrin $\alpha 6$), and *ITGA7* (integrin $\alpha 7$) in OVTW59, SKOV3, and ES-2 cells were determined using real-time RT-PCR analysis. The results were normalized to GAPDH mRNA levels. Data are presented as mean \pm SD ($n = 3$). **D** ConA pull-down assay of integrin $\alpha 3$ and $\alpha 6$. SKOV3 cells were transfected with control siRNA (siControl) or two different *TMTc1* siRNA (siTMTc1-1 or siTMTc1-3). The cell lysates were treated with PNGase F and then pulled down with ConA-agarose beads. integrin $\alpha 3$ was analyzed using Western blotting. GAPDH was used as loading control. OVTW59 cells were transfected with control siRNA (siControl) or *TMTc1* siRNA (siTMTc1-1 or siTMTc1-3).

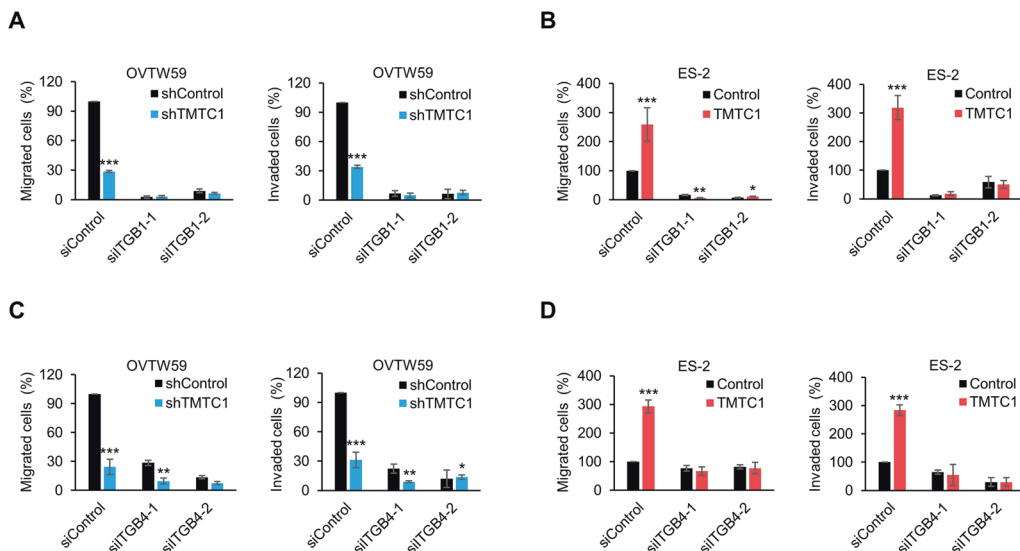


Fig. 5 Integrins $\beta 1$ and $\beta 4$ play a critical role in the *TMTc1*-mediated migration and invasion of ovarian cancer cells. **A** Effects of *TMTc1* knockdown on cell migration and invasion were significantly blocked by *ITGB1* siRNAs in OVTW59 cells. OVTW59 cells stably transfected with the control (shControl) or *TMTc1* knockdown shRNA (shTMTc1) were transiently transfected with *ITGB1* siRNAs (siITGB1-1 and siITGB1-2). Migration and invasion of these cells were analyzed using the Transwell migration assay and Matrigel invasion assay, respectively. $n = 3$. **B** *TMTc1*-increased migration and invasion were significantly reversed in ES-2 cells by *ITGB1* siRNAs. The ES-2 cells stably transfected with the control (Control) or *TMTc1* overexpression vector were transiently transfected with *ITGB1* siRNAs (siITGB1-1 and siITGB1-2). $n = 3$. **C** Effects of *TMTc1* knockdown on cell migration and invasion were significantly blocked in OVTW59 cells by *ITGB4* siRNAs. The OVTW59 cells stably transfected with the control (shControl) or *TMTc1* knockdown (shTMTc1) shRNA were transiently transfected with *ITGB4* siRNAs (siITGB4-1 and siITGB4-2). $n = 3$. **D** *TMTc1*-increased migration and invasion in ES-2 cells were significantly reversed by *ITGB4* siRNAs. ES-2 cells stably transfected with the control (Control) or *TMTc1* overexpression vector (*TMTc1*) were transiently transfected with *ITGB4* siRNAs (siITGB4-1 and siITGB4-2). * $P < 0.05$; ** $P < 0.01$; *** $P < 0.001$. Results are presented as mean \pm SD ($n = 3$). Data were analyzed using the Student's *t*-test.

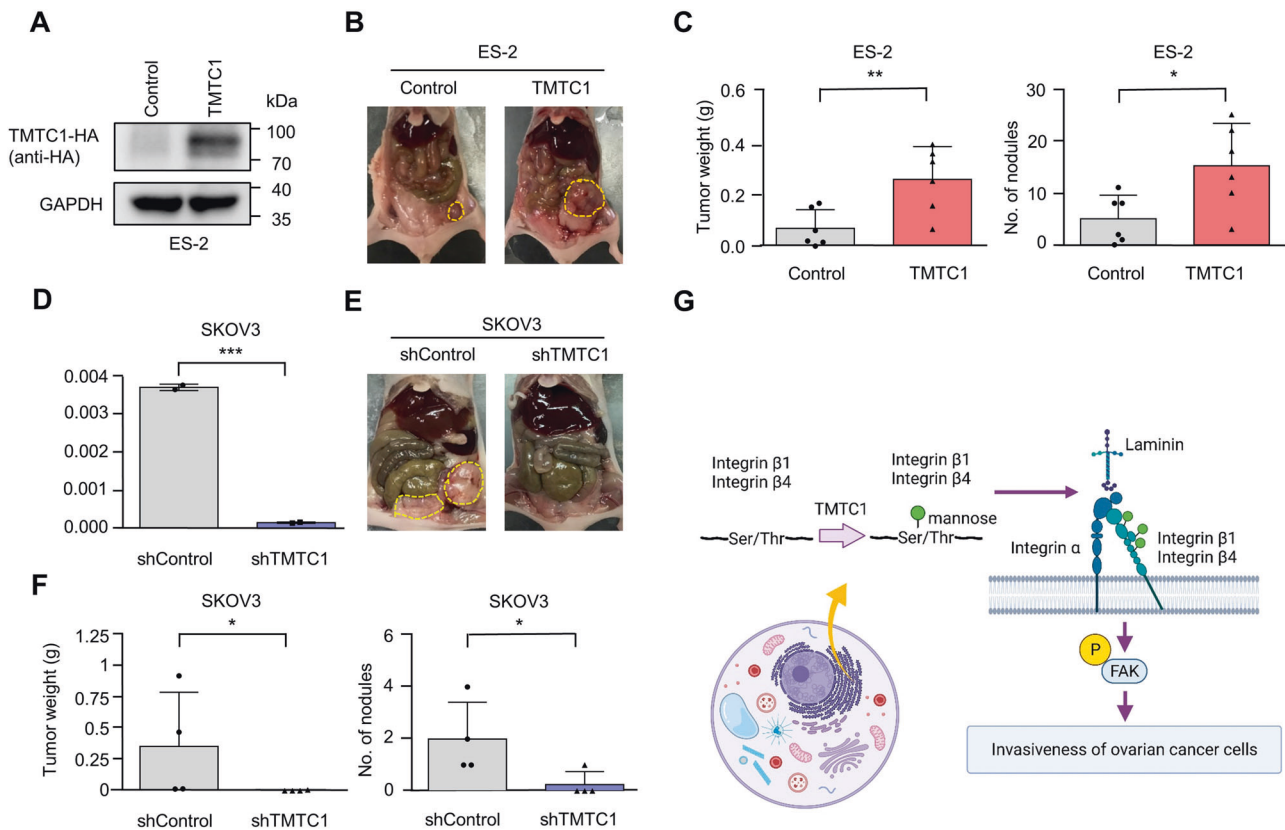


Fig. 6 Effects of *TMTC1* on tumor growth and metastasis *in vivo*. **A** Establishment of *TMTC1*-overexpressing ES-2 cells. HA-tagged *TMTC1* was pulled down using HA tag agarose and then immunoblotted with an anti-HA antibody. **B** Representative images of tumor formation (yellow circles) in nude mice intraperitoneally injected with control or *TMTC1*-overexpressing ES-2 cells. **C** Statistical analyses of tumor weights and nodule numbers from **b**. Mice were sacrificed after injection of cells for 15 days. $n = 6$ for each group. $*P < 0.05$; $**P < 0.01$. Data were analyzed using the Student's *t*-test. **D** *TMTC1* knockdown in SKOV3 cells. The relative transcript levels of *TMTC1* in stable transfectants of SKOV3 cells were measured by real-time RT-PCR and the results were normalized to *GAPDH* mRNA levels. Representative results from three independent experiments were shown. **E** Representative images of tumor formation (yellow circles) in nude mice intraperitoneally injected with the control and *TMTC1* knockdown SKOV3 cells. **F** Statistical analyses of tumor weights and nodule numbers from **d**. Mice were sacrificed after injection of cells for 40 days. $n = 4$ for each group. Data were analyzed using the Mann-Whitney *U* test or one-tailed Student's *t*-test. $*P < 0.05$. **G** A schematic diagram showing the proposed mechanism by which *TMTC1* promotes invasiveness of ovarian cancer cells. *TMTC1* modifies O-mannosylation of integrins $\beta 1$ and $\beta 4$, increasing laminin binding and FAK phosphorylation to promote invasiveness of ovarian cancer cells. This figure was created with BioRender software.

(Fig. 6D). The silencing of *TMTC1* decreased tumor weights and the number of tumor nodules in the peritoneal cavity (Fig. 6E, F). These results suggest that *TMTC1* promotes peritoneal tumor growth and metastasis of ovarian cancer cells.

DISCUSSION

Many patients with ovarian cancer are diagnosed at an advanced stage when the disease has spread throughout the abdominal cavity [1, 2]. To improve patient survival, there is an urgent need to find new therapeutic targets to support the development of agents to inhibit invasion and metastasis. Recently, *TMTC1-4* were identified as novel O-mannosyltransferases with largely unknown protein substrates other than cadherins and protocadherins. Public databases showed that *TMTC1* mRNA is highly expressed in ovarian cancer. Here, we showed that *TMTC1* protein is overexpressed in ovarian cancer and that high expression levels of *TMTC1* are associated with poor prognosis. *TMTC1* promotes ovarian cancer cell growth and invasiveness *in vitro* as well as enhances peritoneal growth and metastasis *in vivo*. Mechanistically, *TMTC1* modulates the O-mannosylation and activity of integrins $\beta 1$ and $\beta 4$ to enhance cell migration and invasion (Fig. 6G). These findings suggest that *TMTC1* is a potential therapeutic

target and advance our understanding of *TMTC1*-mediated O-mannosylation in the pathogenesis of ovarian cancer.

We found that *TMTC1* modifies the O-mannosylation of integrins $\beta 1$ and $\beta 4$ and their downstream signaling molecule p-FAK. Moreover, the *TMTC1*-mediated invasiveness of ovarian cancer cells was significantly reversed by siRNAs of integrin $\beta 1$ or $\beta 4$. Integrins $\beta 1$ and $\beta 4$ are frequently upregulated in ovarian cancer and promote ovarian tumorigenesis and cancer progression [7, 22, 23]. Our results showed that *TMTC1* enhances cell adhesion to laminin and to a lesser extent fibronectin. Moreover, *TMTC1* could slightly modulate the heterodimerization of integrin $\alpha 6$ and $\beta 1$. Within the integrin family of cell adhesion receptors, integrins $\alpha 3\beta 1$, $\alpha 6\beta 1$, $\alpha 6\beta 4$, and $\alpha 7\beta 1$ belong to the laminin-binding subfamily [24]. Previous evidence suggested that integrin $\alpha 6\beta 1$ and $\alpha 6\beta 4$ play important roles in ovarian cancer invasion [25, 26]. Both integrins $\beta 1$ and $\beta 4$ are the β subunit of laminin receptors. Integrin $\beta 1$ is also a part of the main fibronectin receptor $\alpha 5\beta 1$ which also plays a role in ovarian cancer cell invasion [27]. These results strongly suggest that *TMTC1* promotes the invasive behavior of ovarian cancer cells primarily through integrins $\beta 1$ and $\beta 4$.

A broad range of glycosylation alterations in cancer cells, including N-linked and O-linked glycosylation, have been observed. Integrin activities are strongly influenced by glycans

through glycosylation events and glycan-mediated interactions [28]. It is well known that N-glycans on both α and β subunits of integrins can regulate their activities to control cell adhesion and migration [28]. For example, N-glycosylation of integrin $\alpha 5\beta 1$ or $\alpha 6\beta 4$ promotes the complex formation with EGFR and suppresses EGFR signaling pathway for cell growth [29]. We and others have also demonstrated that GalNAc-type O-glycosylation of integrins modulates their functions [5, 8, 30].

Here, we are the first to show the existence of TMTC1-mediated O-mannosylation in integrins $\beta 1$ and $\beta 4$. Moreover, this modification can enhance activities of integrins $\beta 1$ and $\beta 4$ to promote cell-ECM adhesion. Interestingly, our data showed that TMTC1 could not significantly affect the O-mannosylation of integrins $\alpha 3$ and $\alpha 6$, the main α subunits in ovarian cancer cells, as revealed by Con A pull-down assay. This result suggests that TMTC1 exhibits substrate preference toward integrins $\beta 1$ and $\beta 4$. Our data indicate that O-mannosylation occurs in integrin $\beta 1$ and integrin $\beta 4$. We are the first to provide the MS-based evidence demonstrating the existence of O-mannosylation sites on integrins $\beta 1$ and $\beta 4$. It will be of great interest to further investigate the contributions of TMTC1-4 to these sites and the role of site-specific O-mannosylation in integrins.

Besides its function as an O-mannosyltransferase, TMTC1 has been proposed to regulate calcium homeostasis via interaction with SERCA2b [31]. Live cell calcium measurements have revealed that TMTC1 overexpression reduces calcium release from the ER following stimulation. It has been reported that decreased intracellular calcium levels suppress the migration and invasion of ovarian cancer cells [32]. However, our data showed that TMTC1 overexpression promotes migration and invasion. Therefore, the TMTC1-mediated invasiveness of ovarian cancer cells is very unlikely to occur via regulation of calcium levels.

In this study, we showed that TMTC1 is overexpressed in ovarian cancer and is an independent prognostic factor for the prediction of poor outcomes in patients with ovarian cancer. TMTC1 promotes the malignant behaviors of ovarian cancer cells in vitro and in vivo. Notably, silencing of TMTC1 is sufficient to suppress peritoneal tumor growth and dissemination. These findings not only highlight the importance of TMTC1-mediated O-mannosylation in cancer biology but also suggest that TMTC1 could be a potential target for the future development of ovarian cancer therapeutics.

DATA AVAILABILITY

The data that support the findings of our study are available from the corresponding author upon reasonable request.

REFERENCES

- Webb PM, Jordan SJ. Epidemiology of epithelial ovarian cancer. *Best Pr Res Clin Obstet Gynaecol.* 2017;41:3–14.
- Siegel RL, Miller KD, Fuchs HE, Jemal A. Cancer Statistics, 2021. *CA Cancer J Clin.* 2021;71:7–33.
- Hsu WM, Che MI, Liao YF, Chang HH, Chen CH, Huang YM, et al. B4GALNT3 expression predicts a favorable prognosis and suppresses cell migration and invasion via beta(1) integrin signaling in neuroblastoma. *Am J Pathol.* 2011;179:1394–404.
- Chang HH, Chen CH, Chou CH, Liao YF, Huang MJ, Chen YH, et al. beta-1,4-Galactosyltransferase III enhances invasive phenotypes via beta1-integrin and predicts poor prognosis in neuroblastoma. *Clin Cancer Res.* 2013;19:1705–16.
- Liu CH, Hu RH, Huang MJ, Lai IR, Chen CH, Lai HS, et al. C1GALT1 promotes invasive phenotypes of hepatocellular carcinoma cells by modulating integrin beta1 glycosylation and activity. *PLoS One.* 2014;9:e94995.
- Chen CH, Wang SH, Liu CH, Wu YL, Wang WJ, Huang J, et al. beta-1,4-Galactosyltransferase III suppresses beta1 integrin-mediated invasive phenotypes and negatively correlates with metastasis in colorectal cancer. *Carcinogenesis* 2014;35:1258–66.
- Chen CH, Shyu MK, Wang SW, Chou CH, Huang MJ, Lin TC, et al. MUC20 promotes aggressive phenotypes of epithelial ovarian cancer cells via activation of the integrin beta1 pathway. *Gynecol Oncol.* 2016;140:131–7.
- Kuo TC, Wu MH, Yang SH, Chen ST, Hsu TW, Jhuang JY, et al. C1GALT1 high expression is associated with poor survival of patients with pancreatic ductal adenocarcinoma and promotes cell invasiveness through integrin $\alpha 5\beta 1$. *Oncogene* 2021;40:1242–54.
- Neubert P, Strahl S. Protein O-mannosylation in the early secretory pathway. *Curr Opin Cell Biol.* 2016;41:100–8.
- Vester-Christensen MB, Halim A, Joshi HJ, Steentoft C, Bennett EP, Levery SB, et al. Mining the O-mannose glycoproteome reveals cadherins as major O-mannosylated glycoproteins. *Proc Natl Acad Sci USA.* 2013;110:21018–23.
- Larsen ISB, Narimatsu Y, Clausen H, Joshi HJ, Halim A. Multiple distinct O-Mannosylation pathways in eukaryotes. *Curr Opin Struct Biol.* 2019;56:171–8.
- Larsen ISB, Narimatsu Y, Joshi HJ, Siukstaite L, Harrison OJ, Brasch J, et al. Discovery of an O-mannosylation pathway selectively serving cadherins and protocadherins. *Proc Natl Acad Sci USA.* 2017;114:11163–8.
- Larsen ISB, Narimatsu Y, Joshi HJ, Yang Z, Harrison OJ, Brasch J, et al. Mammalian O-mannosylation of cadherins and plexins is independent of protein O-mannosyltransferases 1 and 2. *J Biol Chem.* 2017;292:11586–98.
- Eisenhaber B, Sinha S, Jadalanki CK, Shitov VA, Tan QW, Sirota FL, et al. Conserved sequence motifs in human TMTC1, TMTC2, TMTC3, and TMTC4, new O-mannosyltransferases from the GT-C/PMT clan, are rationalized as ligand binding sites. *Biol Direct.* 2021;16:4.
- Carvalho S, Oliveira T, Bartels MF, Miyoshi E, Pierce M, Taniguchi N, et al. O-mannosylation and N-glycosylation: two coordinated mechanisms regulating the tumour suppressor functions of E-cadherin in cancer. *Oncotarget* 2016;7:65231–46.
- Chen X, Zhang Q, Chekouo T. Filtering high-dimensional methylation marks with extremely small sample size: an application to gastric cancer data. *Front Genet.* 2021;12:705708.
- Makboul R, Abdelkawi IF, Badary DM, Hussein MRA, Rhim JS, Toraih EA, et al. Transmembrane and tetratricopeptide repeat containing 4 is a novel diagnostic marker for prostate cancer with high specificity and sensitivity. *Cells* 2021;10:1029.
- Perez-Riverol Y, Bai J, Bandla C, Garcia-Seisdedos D, Hewapathirana S, Kamatchinathan S, et al. The PRIDE database resources in 2022: a hub for mass spectrometry-based proteomics evidences. *Nucleic Acids Res.* 2022;50:D543–D52.
- Lengyel E. Ovarian cancer development and metastasis. *Am J Pathol.* 2010;177:1053–64.
- Zent R, Pozzi A. Cell-extracellular matrix interactions in cancer. *New York: Springer;* 2010. 314.
- Matulonis UA, Sood AK, Fallowfield L, Howitt BE, Sehouli J, Karlan BY. Ovarian cancer. *Nat Rev Dis Prim.* 2016;2:16061.
- Choi YP, Kim BG, Gao MQ, Kang S, Cho NH. Targeting ILK and beta4 integrin abrogates the invasive potential of ovarian cancer. *Biochem Biophys Res Commun.* 2012;427:642–8.
- Lee JG, Ahn JH, Jin Kim T, Ho Lee J, Choi JH. Mutant p53 promotes ovarian cancer cell adhesion to mesothelial cells via integrin beta4 and Akt signals. *Sci Rep.* 2015;5:12642.
- Arimori T, Miyazaki N, Mihara E, Takizawa M, Taniguchi Y, Cabanas C, et al. Structural mechanism of laminin recognition by integrin. *Nat Commun.* 2021;12:4012.
- Ahmed N, Riley C, Rice G, Quinn M. Role of integrin receptors for fibronectin, collagen and laminin in the regulation of ovarian carcinoma functions in response to a matrix microenvironment. *Clin Exp Metastasis.* 2005;22:391–402.
- Stewart RL, O'Connor KL. Clinical significance of the integrin $\alpha 6\beta 4$ in human malignancies. *Lab Invest.* 2015;95:976–86.
- Kenny HA, Chiang CY, White EA, Schryver EM, Habis M, Romero IL, et al. Mesothelial cells promote early ovarian cancer metastasis through fibronectin secretion. *J Clin Invest.* 2014;124:4614–28.
- Marsico G, Russo L, Quondamatteo F, Pandit A. Glycosylation and integrin regulation in cancer. *Trends Cancer.* 2018;4:537–52.
- Hang Q, Isaji T, Hou S, Zhou Y, Fukuda T, Gu J. N-Glycosylation of integrin $\alpha 5\beta 1$ acts as a switch for EGFR-mediated complex formation of integrin $\alpha 5\beta 1$ to $\alpha 6\beta 4$. *Sci Rep.* 2016;6:33507.
- Zhang C, Deng X, Qiu L, Peng F, Geng S, Shen L, et al. Knockdown of C1GalT1 inhibits radioresistance of human esophageal cancer cells through modifying beta1-integrin glycosylation. *J Cancer.* 2018;9:2666–77.
- Sunryd JC, Cheon B, Graham JB, Giorda KM, Fissore RA, Hebert DN. TMTC1 and TMTC2 are novel endoplasmic reticulum tetratricopeptide repeat-containing adapter proteins involved in calcium homeostasis. *J Biol Chem.* 2014;289:16085–99.
- Liu L, Wu N, Wang Y, Zhang X, Xia B, Tang J, et al. TRPM7 promotes the epithelial-mesenchymal transition in ovarian cancer through the calcium-related PI3K / AKT oncogenic signaling. *J Exp Clin Cancer Res.* 2019;38:106.

ACKNOWLEDGEMENTS

The authors acknowledge the mass spectrometry technical research services from NTU Consortia of Key Technologies and NTU Instrumentation Center. This work was supported in part by the Ministry of Science and Technology, R.O.C. (109-2314-B-002-126 -MY2 to C-HC as well as 108-2320-B-002 -064 -MY3 and 111-2320-B-002 -019 -MY3 to M-CH).

AUTHOR CONTRIBUTIONS

T-CY: validation, investigation, writing—original draft. N-YL: validation. C-YCu: validation, investigation. T-WH: validation, investigation. H-YW: writing—review and editing. H-YL: validation, investigation. C-HC: formal analysis, resources, funding acquisition. M-CH: conceptualization, methodology, writing—review and editing.

COMPETING INTERESTS

The authors declare no competing interests.

ETHICAL APPROVAL

Animal experiments were reviewed and approved by the Institutional Animal Care and Use Committee (IACUC) of College of Medicine, National Taiwan University (IACUC Approval No: 20190377). All mice used in this study were maintained under specific pathogen-free conditions and housed in pathogen-free facilities in a 12 h light/dark cycle with ad libitum access to food and water. Animal studies were conducted in strict accordance with the recommendations in the Guide for the Care and Use of Laboratory Animals.

ADDITIONAL INFORMATION

Supplementary information The online version contains supplementary material available at <https://doi.org/10.1038/s41417-023-00625-y>.

Correspondence and requests for materials should be addressed to Chi-Hau Chen or Min-Chuan Huang.

Reprints and permission information is available at <http://www.nature.com/reprints>

Publisher's note Springer Nature remains neutral with regard to jurisdictional claims in published maps and institutional affiliations.



Open Access This article is licensed under a Creative Commons Attribution 4.0 International License, which permits use, sharing, adaptation, distribution and reproduction in any medium or format, as long as you give appropriate credit to the original author(s) and the source, provide a link to the Creative Commons license, and indicate if changes were made. The images or other third party material in this article are included in the article's Creative Commons license, unless indicated otherwise in a credit line to the material. If material is not included in the article's Creative Commons license and your intended use is not permitted by statutory regulation or exceeds the permitted use, you will need to obtain permission directly from the copyright holder. To view a copy of this license, visit <http://creativecommons.org/licenses/by/4.0/>.

© The Author(s) 2023